Dispersion of the soft E-mode polariton in $BaTiO_3$†

D. Heiman and S. Ushioda
Department of Physics, University of California, Irvine, California 92664
(Received 4 September 1973)

In the Raman spectra of $BaTiO_3$, the soft E-symmetry phonon appears as an overdamped mode with its peak at zero frequency. Numerical fitting of this peak shape to the overdamped harmonic-oscillator model gives the quasiharmonic frequency of 33 cm^{-1} for the right-angle scattering geometry. We have investigated the polariton behavior of this mode by means of near-forward Raman scattering. We found that for small wave vectors the quasiharmonic frequency of the E-mode polariton follows a dispersion curve similar to that for under-damped polaritons in other crystals. From the experimentally obtained dispersion curve of the quasiharmonic frequency, we obtained the value of the static dielectric constant $\epsilon_\perp(0)$ perpendicular to the c axis to be 1250 ± 350. Our present study shows that the soft E mode has the dispersive character appropriate for phonons.

INTRODUCTION

$BaTiO_3$ has been considered a typical "displacive" ferroelectric, and its dielectric as well as lattice-dynamic properties have been the subject of extensive study both theoretically and experimentally. According to the theory of Anderson[1] and Cochran,[2] in a displacive ferroelectric, the dielectric function can be directly related to the lattice normal-mode frequencies via the Lyddane-Sachs-Teller relation, and the ferroelectric transition occurs as a result of the instability of a certain normal mode called the "soft" mode. The soft-mode behavior of one of the phonons in $BaTiO_3$ was observed experimentally by Raman scattering,[3,4] infrared spectroscopy,[5] and inelastic neutron scattering.[6] Thus, it has generally been believed that $BaTiO_3$ is a ferroelectric of the type properly described by the soft-mode theory of Anderson and Cochran.

However, more recent studies indicate that the soft-mode picture of the phase transitions in $BaTiO_3$ may not be complete and that there may be some "order-disorder" character in the behavior of $BaTiO_3$. We are aware of several experimental evidences which suggest this possibility. One of them is the observation made in the diffuse x-ray-scattering pattern by Comes, Lambert, and Guinier.[7,8] They observed sharp streaks in the x-ray patterns and concluded that all phases but the lowest-temperature phase are dynamically disordered and that the observed macroscopic symmetries of the upper temperature phases are only apparent over the average of many ($\sim 10^2$) unit cells. According to this picture, the so-called "overdamped soft E mode," which has been considered the driving phonon of the ferroelectric transition, is actually a tunneling mode of the dynamic disorder even in the ferroelectric phase.

This view of disordered phases is supported by the recent Raman-scattering data in the paraelectric phase obtained by Quittet and Lambert.[9] If the paraelectric phase is truly cubic O_h, first-order Raman scattering is forbidden by symmetry. However, Quittet and Lambert observed first-order Raman scattering above the transition at ≈ 270 and ≈ 520 cm^{-1}, and they interpreted these first-order Raman peaks as induced by disorder and the consequent lowering of local symmetry.

With the disorder picture of the overdamped soft E mode in mind, Shirane *et al.*[10] studied the inelastic neutron scattering from this mode. They found that the mode has an extremely anisotropic dispersion in $\vec{k}$ space, and that the extreme anisotropy of the mode dispersion was sufficient to explain the sharp streaks in the x-ray pattern observed by Lambert *et al.*[7] Their interpretation was that the soft mode indeed has the characteristics of phonons rather than a tunneling mode of the dynamic disorder.

Other evidence that suggests the inadequacy of the soft-mode theory is the discrepancy between the room-temperature static dielectric constant measured at radio frequencies ϵ^{rad} and at far infrared frequencies ϵ^{fir}. The most recent measurement of the dielectric constant at radio frequencies was made by DiDomenico, Wemple, Porto, and Baumen[4]; they obtained the following values:

$$\epsilon_\parallel^{100\ kHz} = 150, \quad \epsilon_\parallel^{250\ MHz} = 80,$$

$$\epsilon_\perp^{100\ kHz} = 3600, \quad \epsilon_\perp^{250\ MHz} = 2300,$$

where $\parallel$ and $\perp$ refer to directions parallel and perpendicular to the tetragonal c axis. The frequency of 250 MHz is high enough to avoid all the piezoelectric resonances and the dielectric constants measured at this frequency should correspond to the clamped static dielectic constant which appears in the Lyddane-Sachs-Teller relation. The static dielectric constant in the far infrared was determined by Barker[5] from the far-infrared reflectivity; he obtained the value

$$\epsilon_\perp^{fir} = 1800 \ .$$

Later, Pinczuk, Burstein, and Ushioda[11] evaluated $\epsilon_{\parallel}^{fir}$ from the polariton dispersion curve of the $A(z)$ modes and obtained the value

$$\epsilon_{\parallel}^{fir} = 38 \pm 6 .$$

More recently, Laghman, Davis and Nakamura[12] reported the value

$$\epsilon_{\perp}^{fir} = 1500$$

based on the fitting of the polariton line shape of the overdamped soft mode. (Here we have interpreted their ϵ_0 to correspond to $\epsilon_{\perp}^{fir}$, but this interpretation may not be appropriate, since they were dealing with oblique polaritons.[13])

A review of these experimental data shows that the static dielectric constant of $BaTiO_3$ measured at far-infrared frequencies ϵ^{fir} is always significantly lower than the radio-frequency values. This observation leads us to believe that there are dipole active excitations whose resonance frequency is below that of the soft E-symmetry phonon at ≈ 33 cm^{-1} at room temperature and that they contribute to the radio-frequency static dielectric constant but not to the far-infrared static dielectric constant. To explain this discrepancy, Chaves and Porto[14] have suggested a model in which relaxation-type oscillators are included to account for the difference.

We carried out the present experiment to learn more about the nature of the overdamped soft E mode in the tetragonal ferroelectric phase and to obtain the far-infrared static dielectric constant $\epsilon_{\perp}^{fir}$ from the dispersion of the soft mode in the polariton regime.[11] In carrying out our experiment, we paid particular attention to the possible detection of effects due to the presence of low-frequency dipole modes or dynamic disorders.

THEORY

The general expression for the Raman cross section is given by

$$\frac{d^2I}{d\Omega\, d\omega} = 4\hbar V \frac{n_s}{n_i} \frac{\omega_s^3 \omega_i}{c^4} \left| b + \frac{a}{4\pi n e^*} \left(\frac{c^2 q^2}{\omega^2} - \epsilon_\infty \right) \right|^2 \times [n(\omega)+1]\, \mathrm{Im}\, [c^2 q^2/\omega^2 - \epsilon(\omega)]^{-1} , \quad (1)$$

where n_i and n_s are the indices of refraction for the incident and scattered light, respectively; ω_i and ω_s are the frequencies of the incident and scattered light, respectively; V is the illuminated volume of the crystal; $n(\omega)$ is the Bose-Einstein thermal factor $n(\omega) = (e^{\hbar\omega/kT} - 1)^{-1}$; and a and b are the atomic displacement and electro-optic susceptibility coefficients, respectively. This result is shown in a recent review article by Mills and Burstein[15] to be equivalent to both the Benson-Mills[16] and the Barker-Loudon[17] theories. Benson and Mills used a Green's-function method to derive a more general form for the scattering cross section which allows the proper self-energy of the TO phonon to enter quite rigorously. Barker and Loudon, on the other hand, based their derivation on the use of the Nyquist or fluctuation-dissipation theorem, where they employ the classical velocity-dependent damping model.

We now need an expression for the dielectric function $\epsilon(\omega)$. Since $BaTiO_3$ has four infrared-active E-symmetry vibrational modes, we would normally write the dielectric function as a sum of five terms, one contribution from the high-frequency electronic background ϵ_∞ and one for each normal mode of vibration. It is convenient to note that at low frequencies the dielectric properties perpendicular to the c axis are due almost entirely to the soft mode. It is known from infrared studies on $BaTiO_3$[5] that the oscillator strength of the soft mode is 10^3 times greater than any other E-symmetry mode. Therefore, at low frequencies we can closely approximate the dielectric properties by a single oscillator model. The frequency-dependent complex dielectric function including velocity-dependent damping is given by

$$\epsilon(\omega) = \epsilon_\infty + \Omega_p^2 / (\omega_{TO}^2 - \omega^2 - i\omega\gamma), \quad (2)$$

where ϵ_∞ is the high-frequency (optical) dielectric constant, ω_{TO} is the zone-center frequency of the soft-TO-phonon branch, and γ is the velocity-dependent damping constant. Ω_p is the ionic plasma frequency defined by

$$\Omega_p^2 = 4\pi n e^*/m ,$$

where e^* and m are the macroscopic effective charge and the effective mass of the mode, respectively, and n is the number of unit cells per unit volume.

Polariton dispersion in the absence of damping is given by

$$c^2 q^2/\omega^2 = \epsilon^0(\omega), \quad (3)$$

where

$$\epsilon^0(\omega) = \epsilon_\infty + \Omega_p^2 / (\omega_{TO}^2 - \omega^2) .$$

Now by defining the solutions of the undamped dispersion relation for the upper and lower branches of the dispersion curve as ω_+ and ω_-, respectively, we get the relation

$$(c^2 q^2 - \omega^2 \epsilon_\infty)(\omega_{TO}^2 - \omega^2) - \omega^2 \Omega_p^2 = (\omega_+^2 - \omega^2)(\omega_-^2 - \omega^2) = 0. \quad (4)$$

Since the high-frequency dielectric constant is much smaller than the low-frequency dielectric constant we can approximate the polariton frequency for the upper branch as $\omega_+^2 = c^2 q^2/\epsilon_\infty$ for the wave vectors considered here. We now need to modify Eq. (1) for our specific experiment. By using identity (4) and the above relation for ω_+ we get for

the last factor in Eq. (1),

$$\mathrm{Im}\left(\frac{c^2q^2}{\omega^2}-\epsilon(\omega)\right)^{-1}=\left(\frac{\omega^2\epsilon_\infty\Omega_p^2}{c^2q^2-\omega^2\epsilon_\infty}\right)\times\left(\frac{\omega\gamma\epsilon_\infty}{(\omega_-^2-\omega^2)^2+\omega^2\gamma^2\epsilon_\infty^2}\right).$$

By substituting this into Eq. (1) and noting that $\Omega_p^2=(\epsilon_0-\epsilon_\infty)\omega_0^2$, since we can also write the dielectric function as

$$\epsilon^0(\omega)=\epsilon_\infty+(\epsilon_0-\epsilon_\infty)\omega_{\mathrm{TO}}^2/(\omega_{\mathrm{TO}}^2-\omega^2),$$

we have for the scattering cross section

$$\frac{d^2I}{d\omega\,d\Omega}\propto\frac{\epsilon_\infty(\epsilon_0-\epsilon_\infty)}{(4\pi ne^*)^2}\left|a+\frac{4\pi ne^*b}{c^2q^2/\omega^2-\epsilon_\infty}\right|^2\times[n(\omega)+1]\left(\frac{\omega_0^2\omega\gamma\epsilon_\infty}{(\omega_-^2-\omega^2)^2+\omega^2\gamma^2\epsilon_\infty^2}\right). \quad (5)$$

It is known from previous work[18] that the term

$$\left|a+\frac{4\pi ne^*b}{c^2q^2/\omega^2-\epsilon_\infty}\right|^2$$

is a slowly varying quantity that modulates the integrated intensity according to the relative contributions of the phonon and photon parts of the polariton. Thus we can replace c^2q^2/ω^2 by $\epsilon^0(\omega)$ and Eq. (5) becomes

$$\frac{d^2I}{d\omega\,d\Omega}\propto\frac{\epsilon_\infty(\epsilon_0-\epsilon_\infty)}{(4\pi ne^*)^2}\left|a+\frac{4\pi ne^*b}{\Omega_p^2}(\omega_{\mathrm{TO}}^2-\omega_-^2)\right|^2\times[n(\omega)+1]\left(\frac{\omega_{\mathrm{TO}}^2\omega\,\omega_-\Gamma}{(\omega_-^2-\omega^2)^2+4\omega_-^2\omega^2\Gamma^2}\right), \quad (6)$$

where we have defined the dimensionless damping parameter $\Gamma=\gamma\epsilon_\infty/2\omega_-$.

We note that since the third and fourth factors in Eq. (6) are the only ones that contain ω, they will determine the line shape, while the second factor determines the variation in the integrated intensity of the scattered light.

The polariton wave vector $\vec{q}$ is determined by the energy and momentum conservation relations

$$\omega_i=\omega_s+\omega, \quad \vec{k}_i=\vec{k}_s+\vec{q}$$

for the Stokes component, where $\vec{k}_i$ and $\vec{k}_s$ are the wave vectors of the incident and scattered light, and ω_i and ω_s are the frequencies of the incident and scattered light, respectively. For the case of small scattering angles θ between $\vec{k}_i$ and $\vec{k}_s$ inside the crystal, we have, for the crystal momentum

$$c^2q^2=\left\{\omega_i(n_i-n_s)+\omega\left[n_s+\omega_i\left(\frac{\partial n_s}{\partial\omega}\right)\right]\right\}^2+\omega_i^2n_in_s\theta^2, \quad (7)$$

where n_i and n_s are the indices of refraction for the incident and scattered light, respectively. The Raman-tensor elements for the crystal symmetry class C_{4v} as given by Loudon[19] for the E-symmetry modes are

$$E(x)=\begin{pmatrix}0&0&e\\0&0&0\\e&0&0\end{pmatrix}$$

and

$$E(y)=\begin{pmatrix}0&0&0\\0&0&e\\0&e&0\end{pmatrix}.$$

Thus, in order to get a pure symmetry mode, either the incident or scattered light must be parallel to the [001] axis. For our experiment we chose the incident light to be polarized in the [010] direction while the scattered light was polarized in the [001] direction. Now the index of refraction for the incident light is that for the ordinary ray ($n_i=n_o$) and the index of refraction for the scattered light is that for the extraordinary ray ($n_s=n_e$). Since the birefringence is large, $n_o-n_e\cong 0.06$, we can neglect the term proportional to ω, and now Eq. (7) reduces to

$$c^2q^2=\omega_i^2[(n_o-n_e)^2+n_en_o\theta^2]. \quad (8)$$

For the particular scattering geometry used in our experiment, we can see from Eq. (8) that the minimum value of the wave vector, even for extremely small angles ($\theta\sim 0^\circ$), is determined by the amount of birefringence. Thus using for the indices of refraction:

$$n_o=2.488, \quad n_e=2.242 \text{ at } 5145\ \text{Å}$$

and

$$n_o=2.412, \quad n_e=2.360 \text{ at } 6328\ \text{Å}$$

as measured by Wemple *et al.*[20] on a melt-grown crystal of similar quality to the present sample, the lower limits on the wave vector are

$$cq=820\ \mathrm{cm}^{-1} \quad \text{at } 6328\ \text{Å}$$

and

$$cq=1230\ \mathrm{cm}^{-1} \quad \text{at } 5145\ \text{Å}.$$

EXPERIMENTAL

Two exciting sources were available, a 40-mW He-Ne laser operating at 6328 Å and a 50-mW argon-ion laser operating at 5145 Å. The He-Ne laser was used to explore the region of small wave vector by taking advantage of the small birefringence at this wavelength. For larger wave vectors ($cq>1300\ \mathrm{cm}^{-1}$) the argon-ion laser was used since the scattering efficiency is greater and our photomultiplier (ITT FW130) with S-20 surface is much more efficient at this wavelength.

All measurements were made at room temperature on a commercially available melt-grown sample that had been properly poled to remove all 90° domains. The laser was focused into the $BaTiO_3$

single crystal (~5-mm cube) by a 100-cm-focal-length lens. This gave a convergence angle of the incident light $2\Delta\theta_i \lesssim 0.04°$ inside the crystal. The scattered light was collected by a 34-cm-focal-length lens and dispersed by a Spex model-1400 double-grating monochrometer. Since the soft mode is centered about the laser frequency, very narrow spectrometer slits ($< \frac{1}{2}$ cm^{-1}) were employed, enabling us to measure the Raman spectrum to within 5 cm^{-1} of the exciting frequency. The acceptance angle of the collection optics for the scattered light was defined to be $2\Delta\theta_s \lesssim 0.08°$ inside the crystal by placing a 1-mm slit in front of the first collection lens. The light scattered between $\theta = 0°$ and $\theta = 3°$ relative to the incident beam inside the crystal passed through a polarization analyzer and then was frequency analyzed by the spectrometer. Recording of the spectra was accomplished by photon-counting techniques. A PDP-11 minicomputer was interfaced with the spectrometer, photomultiplier, and teletype control as described by Ushioda, Valdez, Ward, and Evans.[21] The computer was programmed to control the stepping motor attached to the spectrometer and to store the digital output from the photomultiplier in its memory. The computer was also programmed to record the data on a paper tape for direct transfer to a larger computer for numerical processing of the spectra.

The experimental scattering geometry employed was $X(YZ)X + \Delta Y$. This means that the light was incident in the X direction [100] with Y polarization [010] and the collected light was scattered in the X direction with Z polarization [001]. Thus the incident polarization was ordinary and the scattered polarization was extraordinary. The ΔY refers to the direction in which the scattered light was deviated slightly from the forward direction. The large birefringence of $BaTiO_3$ causes the incident and scattered wave vectors to differ greatly in magnitude and for small scattering angles the phonon wave vector will also lie in nearly the same direction. By using different laser sources and keeping the scattering angle small, the phonon wave vector was maintained in a [100] direction.

Data taken with the He-Ne laser were difficult to analyze due to the presence of grating ghosts and low signal-to-noise ratio. In some of the weak spectra where the signal-to-noise ratio was small (~4), accurate knowledge of the background intensity was essential. For weak spectra the values of the fitting parameters were found to depend on the relative signal strength from the soft mode, hence the total background must be subtracted from the line shape before any analytic fitting can be performed.

Figure 1 shows how the Raman line shape changes as the scattering wave vector changes. The Raman

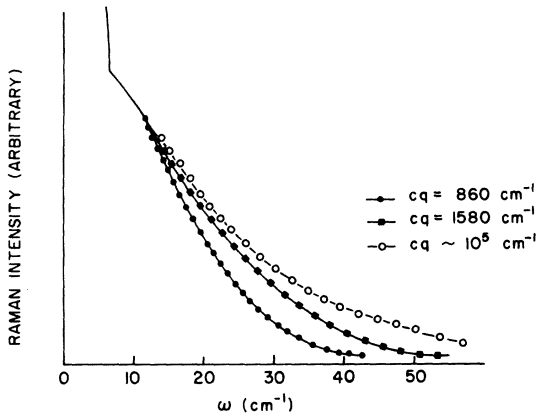

FIG. 1. Raman intensity vs ω for the soft E-symmetry mode. The three curves show how the Stokes line shape changes as a function of wave vector. The open circles show the line shape for long-wavelength back scattering while the solid squares and solid circles are for smaller wave vectors of $cq = 1580$ cm^{-1} and $cq = 860$ cm^{-1}, respectively. Note that the amplitudes were separately adjusted so that they all were of equal amplitude at small frequency.

line shapes for all wave vectors were fit to the analytic formula

$$I(\omega) = I_0[n(\omega)+1]\frac{\omega_{TO}^2\,\omega\,\omega_-\Gamma}{(\omega_-^2-\omega^2)^2+4\omega_-^2\omega^2\Gamma^2}, \tag{9}$$

where

$$I_0 \propto \left| a + \frac{4\pi n e^* b}{\Omega_p^2}(\omega_{TO}^2 - \omega_-^2)\right|^2$$

according to Eq. (6). We obtained the values of I_0, ω_-, and Γ for each $\vec{q}$ value by fitting Eq. (9) to the data points, treating I_0, ω_-, and Γ as adjustable parameters. The values of I_0 and ω_- determined by the best fit for each spectrum are plotted in Figs. 3 and 4, respectively. Spectra for all wave vectors could be fit to this analytic form. Figure 2 shows the experimental data plotted along with the best-fit theoretical curve for the parameters $\omega_- = 19$ cm^{-1} and $\Gamma = 0.77$ for the smallest wave vector examined of $cq = 860$ cm^{-1}. In searching the best-fit values of the parameters I_0, ω_-, and Γ, we started the fitting process with different combinations of the starting values for I_0, ω_-, and Γ. The final values reached by these parameters for the best fit were identical and independent of the starting combinations. The values of I_0, ω_-, and Γ seem to be weakly correlated, and the error caused by the correlation is within the error bars shown in the figures.

Figure 3 shows a plot of the integrated intensity I_0 as a function of $(\omega_{TO}^2 - \omega_-^2)$. Since the intensity increased as ω_- decreases, we conclude that the contributions from both the displacive and electro-

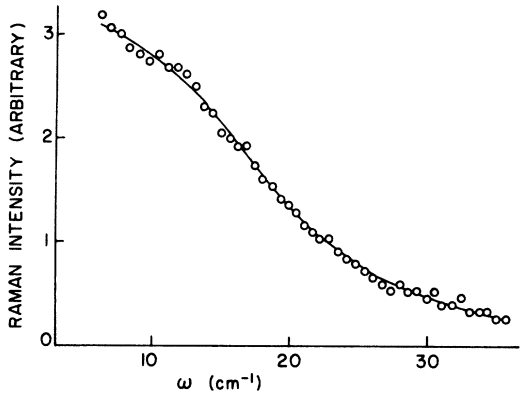

FIG. 2. Raman intensity vs ω for a polariton of wave vector of $cq = 850$ cm^{-1}. The open circles represent the data points while the solid curve represents the best-fit analytic function for $\omega_- = 19$ cm^{-1} and $\Gamma = 0.77$.

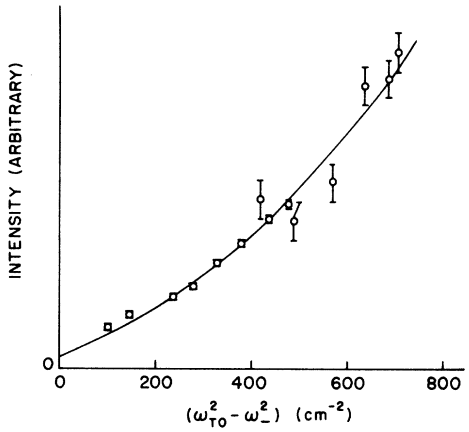

FIG. 3. Integrated intensity I_0 vs $(\omega_{TO}^2 - \omega_-^2)$ for the soft E-mode polariton. The open circles represent the experimental data points with error bars resulting from the uncertainty in the analytic fit for I_0. The solid line represents the best fit of the appropriate analytic formula where each point is weighted by the reciprocal of the uncertainty.

optical terms are of the same sign. From the variation of the integrated intensity I_0 with $(\omega_{TO}^2 - \omega_-^2)$, we were able to find the experimental value

$$4\pi ne^* b/a = +6200 \pm 200 .$$

Although the variation of Γ as a function of ω_- was not found to be conclusive, it appears that Γ is approximately proportional to ω_-, or that the velocity dependent damping constant γ is proportional to ω_-^2. The pure-E-mode polariton did not become underdamped even for the smallest value of q which was reached in our experiment.

Now by plotting the quasiharmonic frequency ω_- as a function of the wave vector cq in Fig. 4, we find that it has a dispersion character similar to that for underdamped polaritons in other crystals. Assuming that the soft mode accounts for nearly all of the dielectric properties at these low frequencies, the dispersion curve was found to fit an undamped single-oscillator model of the form

$$\frac{c^2q^2}{\omega_-^2} = \epsilon_{\perp\infty} + \frac{[\epsilon_\perp(0) - \epsilon_{\perp\infty}]\omega_{TO}^2}{\omega_{TO}^2 - \omega_-^2} ,$$

using $\epsilon_{\perp\infty} = 5.22$ and the value we determined for the transverse optic mode frequency $\omega_{TO} = 33$ cm^{-1}. A good fit to this function was obtained as shown in Fig. 4 using $\epsilon_\perp(0)$ as the adjustable parameter which resulted in a value for the low-frequency dielectric constant of

$$\epsilon_\perp(0) = 1250 \pm 350 .$$

DISCUSSION

From Fig. 4 we can see qualitatively that the soft quasiharmonic mode frequency ω_- does have a dispersive character which depends on the polariton wave vector. We note that this dispersion is very similar to that for polaritons in other crystals.[22]

This definite dependence on wave vector implies that there is a long-range macroscopic correlation associated with the intense low-frequency scattering, since there is obvious momentum or wave-vector conservation in this process. This long-range correlation supports the collective vibrational character picture or phonon model in agreement with the conclusion reached by Shirane *et al.*[10]

From the quantitative behavior of the quasiharmonic mode frequency dispersion, we were able to fit the experimental data with an undamped single oscillator model for the dielectric function. From

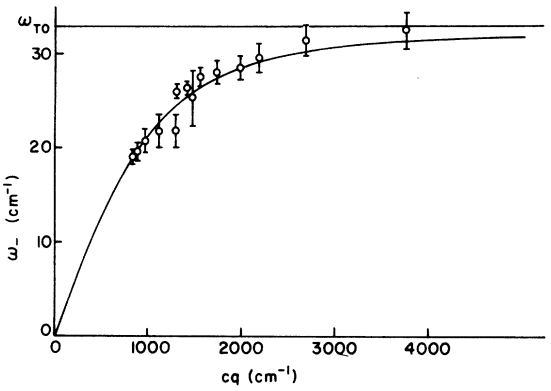

FIG. 4. Dispersion of the quasimode frequency ω_- vs wave vector cq for the soft E-mode polariton. The open circles represent the experimental data taken with two different laser sources. The solid curve is the theoretical fit of an undamped dielectric function for a single oscillator model using $\epsilon(0) = 1250$.

this we obtained a value for the low-frequency dielectric constant of $\epsilon_\perp(0) = 1250 \pm 350$. We note that this does not give a very accurate value of $\epsilon_\perp(0)$ due to the inability to measure ω_- at very small wave vectors, but it does give an approximate value for the low-frequency (far-infrared) dielectric constant in the 10-cm^{-1} range. Although we have no direct measurement of the dielectric constant at far-infrared frequencies on our melt-grown crystal we might examine that for flux-grown crystals. Even though it is known that the dielectric properties differ due to the method of growth we can still get some indication of the dielectric constant at far infrared frequencies. Berlincount and Jaffe[23] give the free and clamped values for their flux-grown sample as

$$\epsilon_\perp(0) = 2900 \text{ at } 1 \text{ MHz}$$

and

$$\epsilon_\perp(0) = 2000 \text{ at } 20\text{–}30 \text{ MHz},$$

respectively. Benedict and Durand[24] found the value to be

$$\epsilon_\perp(0) \approx 2000 \text{ at } 1 \text{ cm}^{-1}.$$

From these data we may conclude that there is no appreciable dispersion of the clamped dielectric constant in the high radio-frequency region. The clamped value appropriate to our melt-grown sample is

$$\epsilon_\perp(0) = 2300 \text{ at } 250 \text{ MHz}$$

as reported by DiDomenico *et al.*[2] Our value of $\epsilon_\perp(0)$ only accounts for half of the measured clamped dielectric constant. A similar situation exists for $\epsilon_\parallel(0)$ derived from the $A(z)$ symmetry modes of $BaTiO_3$. The value of $\epsilon_\parallel(0)$ obtained from both the Lyddane-Sachs-Teller relation and from the polariton-dispersion curve also can only account for about one-half of the measured value of the clamped dielectric constant.[11] This leads us to believe that there may be other excitations in the frequency range 1–10 cm^{-1} that account for the additional dielectric contributions.

From the variation of the integrated intensity I_0 with the polariton quasiharmonic mode frequency ω_-, we were able to obtain the value for the ratio $4\pi ne^*b/a$. We now write the Raman scattering tensor as[18]

$$\chi' = \left(\frac{\partial\chi}{\partial u}\right)_E u + \left(\frac{\partial\chi}{\partial E}\right)_u E = \chi'(u) + \chi'(E),$$

where χ is the electric susceptibility tensor, and u and E refer to the atomic displacement and the electric field of the polariton, respectively. We can now relate the ratio $4\pi ne^*b/a$ to the ratio of the electro-optic and the displacive contributions

$$4\pi ne^*b/a \propto \chi'(E)/\chi'(u).$$

Thus, we can see from the very large ratio of 6200 that the scattering is due primarily to the electro-optic contribution rather than the displacive contribution. We can compare our value of $4\pi ne^*b/a$ to that of other crystals. Crystals of the zinc-blende and wurtzite structure have typical values on the order of 10.[18] Thus, the relative electro-optic contribution to the soft E mode in $BaTiO_3$ is huge by comparison.

We noted that the damping of the polariton decreased as the quasiharmonic frequency decreased roughly linearly. Thus, even though we only observed the mode to be overdamped ($\Gamma > 0.77$), we may speculate that at smaller values of the polariton wave vector that we were unable to obtain, that the mode will become underdamped as observed by Laughman *et al.*[12]

CONCLUSION

We measured the Raman spectra of the soft E mode in $BaTiO_3$ in the polariton regime. Although this mode is overdamped and the Raman spectra for experimentally accessible wave-vector values show no peak, we could obtain the quasiharmonic mode frequency ω_- as a function of the wave vector $\vec{q}$ by means of numerical analysis of the spectra. The dispersion of ω_- can be adequately described by a frequency-dependent dielectric function based on a single oscillator model. From the dispersion of ω_-, we obtained the value of the static dielectric constant $\epsilon_\perp(0) = 1250 \pm 350$. The fact that the wave vector of the mode $\vec{q}$ is well defined near $\vec{q} = 0$ shows that this mode has the phonon character with a long-range correlation of the atomic displacements.

From the variation of the scattering intensity as a function of the wave vector, we obtained the ratio between the electro-optic and displacive contributions to the Raman scattering intensity, and found that the electro-optic contribution is much greater than the displacive contribution.

Note added in proof. On closer study of Ref. 12, we found that the mode observed by Laughman, Davis, and Nakamura is not oblique polariton but pure E-symmetry polariton.

ACKNOWLEDGMENTS

We wish to acknowledge our gratitude for the many helpful discussions with Professor D. L. Mills. One of us (D. H.) also wishes to express thanks to J. D. McMullen for his guidance throughout the experiment.

†Research supported by the Air Force Office of Scientific Research, Air Force Systems Command, USAF, under Grant No. AFOSR-72-2296, Technical Report No. 73-60.

[1]P. Anderson, in *Proceedings of the All-Union Conference on the Physics of Dielectrics* (Academy of Sciences USSR, Moscow, 1958), p. 290.
[2]W. Cochran, Adv. Phys. 9, 387 (1960).
[3]M. DiDomenico, Jr., S. P. S. Porto, and S. H. Wemple, Phys. Rev. Lett. 19, 855 (1967).
[4]M. DiDomenico, Jr., S. H. Wemple, S. P. S. Porto, and R. P. Bauman, Phys. Rev. 174, 522 (1968).
[5]A. S. Barker, Jr., Phys. Rev. 145, 391 (1966).
[6]G. Shirane, B. C. Frazer, V. J. Minkiewicz, J. A. Leake, and A. Linz, Phys. Rev. Lett. 19, 234 (1967).
[7]R. Comes, M. Lambert, and A. Guinier, Solid State Commun. 6, 715 (1968).
[8]M. Lambert and R. Comes, Solid State Commun. 7, 305 (1969).
[9]A. M. Quittet and M. Lambert, Solid State Commun. 12, 1053 (1973).
[10]G. Shirane, J. D. Axe, and J. Harada, Phys. Rev. B 2, 3651 (1970).
[11]A. Pinczuk, E. Burstein, and S. Ushioda, Solid State Commun. 7, 139 (1969).
[12]L. Laughman, L. W. Davis, and Terutaro Nakamura, Phys. Rev. B 6, 3322 (1972).
[13]W. S. Otaguro, E. Wiener-Avnear, S. P. S. Porto, and J. Smit, Phys. Rev. B 6, 3100 (1972).
[14]A. S. Chaves and S. P. S. Porto (unpublished).
[15]D. L. Mills and E. Burstein (unpublished).
[16]H. J. Benson and D. L. Mills, Phys. Rev. B 1, 4835 (1970).
[17]A. S. Barker and R. Loudon, Rev. Mod. Phys. 44, 18 (1972).
[18]S. Ushioda, A. Pinczuk, E. Burstein and D. L. Mills, *Light Scattering Spectra of Solids*, edited by G. B. Wright (Springer, New York, 1969), p. 347.
[19]R. Loudon, Adv. Phys. 13, 423 (1964).
[20]S. H. Wemple, M. DiDomenico, Jr., and I. Camblibel, J. Phys. Chem. Solids 29, 1797 (1968).
[21]S. Ushioda, J. B. Valdez, W. H. Ward, and A. R. Evans, Rev. Sci. Instr. (to be published).
[22]C. H. Henry and J. J. Hopfield, Phys. Rev. Lett. 15, 964 (1965).
[23]Don Berlincount and Hans Jaffe, Phys. Rev. 111, 143 (1958).
[24]T. S. Benedict and J. L. Durand, Phys. Rev. 109, 1091 (1958).